

# Design of formation and appropriate coordinate expression along general elliptic orbit using regularization

R. Funase and J. Kawaguchi

## Abstract

This paper deals with how the formation flight target is expressed as trivial and fixed in some appropriate coordinates, instead of an orbital target. This fixed bin/slot property is essential for the formation maintenance control. A new coordinate transformation is introduced for the case of circular reference trajectory, and compared with conventional C-W coordinate, the advantage of the new coordinate transformation is shown in terms of control performance index and formation maintenance property. Then, the discussion is extended to the case of general elliptic reference orbit, where regularization and Levi-Civita non-linear coordinate transform is introduced as a formation design methodology. Pseudo-constant distance formation around elliptic orbit is designed as an example and the effectiveness of the proposed method is numerically verified.

## 1. Introduction

The formation flying along circular trajectories has been well developed and also well known, and a lot of investigations have been carried out. The most familiar approach to the dynamics is to use so called the Hill's equation or, in other words, the C-W equation, in which the linearized motion is described as a set of ordinary differential equations with constant coefficients. Its in-plane motion is expressed as:

$$\ddot{x} - 2n\dot{y} - 3n^2x = u, \quad \ddot{y} + 2n\dot{x} = v \quad (1)$$

As long as the initial-value problem is concerned, the transient behavior is explicitly written and the asymptotic stability is easily verified in this approach, when a conventional feedback scheme with steady constant gains is introduced in the Hill's coordinate domain. However, in the actual formation control applications, the target to be traced and maintained is persistently moving along with time. The equations of motion associated with circular trajectories naturally contain the 0-th order derivative term, and maintaining the formation inevitably, in most cases, requires a certain feedforward acceleration control to be input. It is true that the residual error vanishes once

the feed-forward control strategy is incorporated. However, even though the stability is assured with no residual error, there are still some aspects to be examined for practical use.

This paper first discusses the appropriate coordinate expression for different kind of formation flying missions, where a formation around circular orbit is assumed and three different coordinates are presented and evaluated; 1) C-W coordinate, 2) Inertial coordinate and 3) p-coordinate that is newly introduced, and the p-coordinate is shown effective for a formation where each spacecraft is moving on a locus in the C-W coordinate. Then, the discussion is extended to the formation around general elliptic orbit. The design of formation is not so simple as for the case of circular trajectory. Here, the technique of regularization and some coordinate transformation is introduced to enable comprehensive formation design around elliptic orbit. As an example, a constant distance formation is derived by using the transformation.

## 2. Coordinates for formation expression

The C-W equation (eq.(1)) is converted to an alternative expression corresponding to the inertial motion, and the following equation:

$$\ddot{q} + F(\theta)q = U \quad (2)$$

is obtained, where

$$F(\theta) = n^2 \begin{pmatrix} 1 - 3\cos^2 \theta & -3\sin \theta \cos \theta \\ -3\sin \theta \cos \theta & 1 - 3\sin^2 \theta \end{pmatrix} \quad (3)$$

and  $\theta$  is true-anomaly of the reference spacecraft. It is a time-varying system with a periodic coefficient matrix  $F$  in it. It is not straightforward to verify if the feedback control is stable, and the closed system may result in steady state bias unless an appropriate feed-forward control is introduced, since it contains the 0-th order derivative term. But the use of this inertial coordinate is objectively suitable for some applications such as astronomy missions, which require the control performance property defined in inertial space.

There is still another aspect in the formation flying. What the formation target should be depends on the control objective, and it might be worthy referring to the special case, in which the formation motion is expressed by the following time-varying equation, in which no 0-th order derivative term appears. We call the new expression ‘‘p-coordinate.’’

When a contraction of  $x' = x$ ,  $y' = y/2$  is used, and the rotation coordinate transformation of

$$p = \begin{pmatrix} \xi \\ \eta \end{pmatrix} = \begin{pmatrix} \cos \theta & -\sin \theta \\ \sin \theta & \cos \theta \end{pmatrix} \begin{pmatrix} x' \\ y' \end{pmatrix} \quad (4)$$

is introduced (see Fig. 1), the equations of motion is altered to the following time-varying expression.

$$\ddot{p} + A(\theta)\dot{p} = \begin{pmatrix} \cos \theta & -\sin \theta \\ \sin \theta & \cos \theta \end{pmatrix} \begin{pmatrix} u \\ \frac{1}{2}v \end{pmatrix} = \hat{U} \quad (5)$$

where

$$A(\theta) = n \begin{pmatrix} 3 \sin \theta \cos \theta & 1 - 3 \cos^2 \theta \\ -1 + 3 \sin^2 \theta & -3 \sin \theta \cos \theta \end{pmatrix} \quad (6)$$

It is clear that a trivial solution, a constant vector always satisfies the equation above. This corresponds to the state in which the formation is frozen along similar ellipse trajectories, i.e. like cart wheel orbits.

Here p-vector denotes the transformed state vectors along a circular trajectory. An importance of the form above is in the direct / trivial provision of the steady state solution that satisfies them automatically. At the cost of non-autonomy, the modified equations here show some advantages especially for the formation maintenance guidance and control, without relying on the feed-forward efforts. The formation maintenance has only to result in controlling the spacecraft position into a virtual bin or slot defined in this p-coordinate. The relative approach trajectory is handled much more easily with the equations, whose transition matrix is also depicted in the paper.

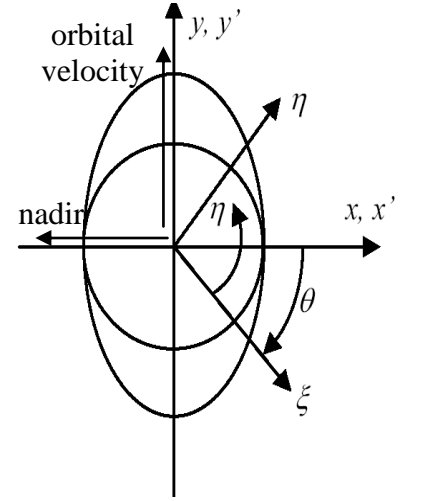


Fig. 1: *p*-Coordinate

As seen in this formation flight, here, no feed forward acceleration input is required apparently to maintain the formation. The paper presents the stability criterion and other properties for the feedback control scheme to this case. The discussion, at the same time, presents the convergence property to the target, either a bin or a slot to which each spacecraft shall be controlled. Note regardless of selection of coordinates, the dynamics itself never changes and what is seen and observed is just apparent behavior with artificial control input.

### 3. Merit of conversion to non-autonomous system

In this section, the merit of the introduction of non-autonomous expression (inertial and p-coordinates) by comparing with the autonomous expression (CW coordinate).

This section simply points out that the use of the C-W equation may degrade the convergence performance in the applications that intend the relative geometry to be pointed to the

inertial target, simply because the C-W equation is not necessarily suitable for that purpose. This degradation is accounted for either from the performance index point of view that directionally weights the formation accuracy, or from the altered dynamics structural point of view. Needless to say, the stability needs to be looked at from the time-varying motion's point of view.

Fig. 2 is a diagram which shows the relation between the C-W dynamics domain and the time-varying formation domain. What is usually discussed is inside the dotted block, the C-W dynamics, in which the stability is examined easily. However, the formation of concern is associated with the time-varying property that is modulated not only periodically but sometimes in terms of size and scale. This thing corresponds to the formation maintenance allowance that is directionally different. For instance, the focal length / longitudinal tolerance is much more vigorous than lateral control tolerance. How the controller performance is affected is examined in this section. Designing the controller has to take this characteristic into account, and might result in the time-varying feed-back strategy for better performance, such as based on the periodic Riccati matrix solution in time-varying Linear Quadratic problem.

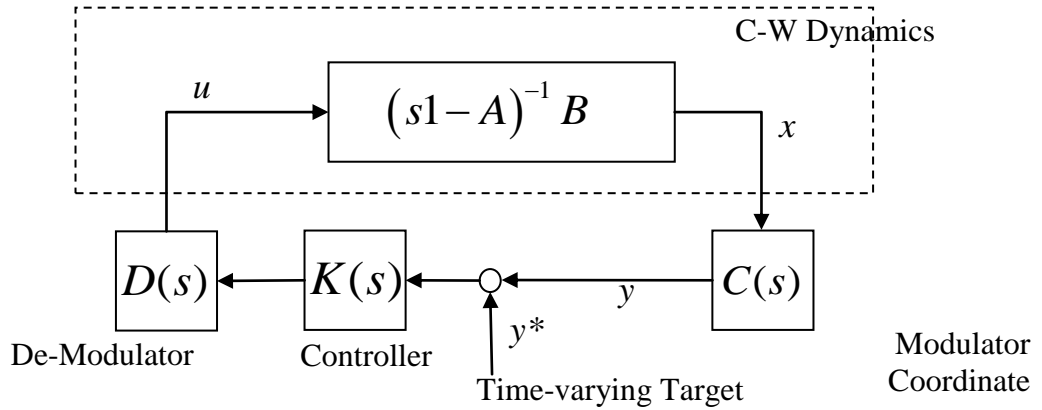


Fig. 2: Control System Transfer Function Characteristics

### 3.1 Stability and controller stability of non-autonomous system

Provided an autonomous system describing the formation motion is given as

$$\dot{x} = Ax + Bu \quad (7)$$

when time-varying and projection mapping transformation of

$$\hat{x} = \Theta(t)Px, \quad x = P^{-1}\Theta(t)^T \hat{x} \quad (8)$$

is introduced, an altered system is described by the following non-autonomous system.

$$\dot{\hat{x}} = \{\Theta PAP^{-1}\Theta^T - [\omega]\} \hat{x} + \Theta PBu = \hat{A}(t)\hat{x} + \hat{B}(t)u \quad (9)$$

With the control input combining both Feed-Forward and Feedback Laws of

$$u = u^* - K(t)(\hat{x} - \hat{x}(t)^*) \quad (10)$$

where  $u^*$  satisfies

$$\dot{\hat{x}}(t)^* = \hat{A}(t)\hat{x}(t)^* + \hat{B}(t)u^* \quad (11)$$

the state error  $\Delta\hat{x} = \hat{x} - \hat{x}(t)^*$  behaves according to

$$\Delta\dot{\hat{x}} = \{\hat{A}(t) - \hat{B}(t)K(t)\}\Delta\hat{x} \quad (12)$$

If the stability above converging to the origin is verified in some manner, there is no steady state residual. It should be noted that this is not straight-forward in Non-Autonomous systems.

Here are summarized typical characteristics in using three coordinates:

(1) Hill's Coordinate

Stability is verified through conventional eigen values. Solutions are available analytically .

(2) Inertia Coordinate

Stability is verified via examining Lyapunov property. Solutions are available analytically.

$$\ddot{q} + F(\theta)q = U, \quad U = -c\dot{q} - (K - F(\theta))q \quad (13)$$

(3) p-Coordinate:

Stability is verified via examining Lyapunov property. Solutions are available analytically.

$$\ddot{p} + A(\theta)\dot{p} = \hat{U}, \quad U = -c\dot{p} - Kp \quad (14)$$

The control laws shown above are some examples.

### 3.2 How non-autonomous description works

There is no direct distinction among three coordinates, since the dynamics never changes, and the stability and avoiding steady state residual are feasibly assured for each description. However, the paper dares to present two aspects on how such non-autonomous description works. What follows lists the subsequent major topics elaborated.

1. Distinction is depicted between C-W and inertial coordinates in terms of performance index associated with the control laws. Discussion also looks at the attitude control aspect, in which control thrust had better be applied along inertial axes.
2. Distinction is shown for p-Coordinate, when the formation maintenance is intended with no Feed-Forward acceleration.

#### Controller performance distinction

Assuming an appropriate Feed-Forward compensation is properly applied, and provided an autonomous system is given as

$$\dot{x} = Ax + Bu \quad (15)$$

With the rotation transformation of  $\hat{x} = \Theta(t)x$ ,  $x = \Theta(t)^T \hat{x}$ , the following non-autonomous system is obtained.

$$\dot{\hat{x}} = \left\{ \Theta A \Theta^T - [\omega] \right\} \hat{x} + \Theta B u = \hat{A}(t) \hat{x} + \hat{B}(t) u \quad (16)$$

Here is assumed the Performance Index (criterion) written as a function of linear quadratic products as

$$\hat{J} = \int_0^\infty \left( \frac{1}{2} \hat{x}^T \hat{Q} \hat{x} + \frac{1}{2} u^T R u \right) \quad (17)$$

to have a feed-back law taking the form of  $u = -\hat{K} \hat{x}$ . This is the most straightforward controller design contemporarily taken. Below are summarized how the performance is evaluated under the feedback law adopted.

#### Case-1: Use of Non-Autonomous Dynamics with Steady LQ Criterion

Under the Non-Autonomous system of

$$\dot{\hat{x}} = \left\{ \Theta A \Theta^T - [\omega] \right\} \hat{x} + \Theta B u = \hat{A}(t) \hat{x} + \hat{B}(t) u \quad (18)$$

with the Performance Index (criterion):

$$\hat{J} = \int_0^\infty \left( \frac{1}{2} \hat{x}^T \hat{Q} \hat{x} + \frac{1}{2} u^T R u \right) \quad (19)$$

to have a Feed-Back law of  $u = -\hat{K} \hat{x}$ .

#### Case-2: Use of Autonomous Dynamics with Time-Varying LQ Weighting

Under the Autonomous system:

$$\dot{x} = A x + B u$$

with the Performance Index (criterion):

$$\hat{J} = \int_0^\infty \left( \frac{1}{2} x^T \left( \Theta(t)^T \hat{Q} \Theta(t) \right) x + \frac{1}{2} u^T R u \right) \quad (20)$$

to have a Feed-Back law of  $u = -\hat{K} \Theta(t) x$ .

It should be noted that two alternative interpretations above are basically identical, but that these will provide useful properties that can identify the difference in controllers performance between C-W and Inertial coordinates.

#### Case-1: Transfer Function Distinction

Suppose  $\lambda_A$  is an eigen value of matrix A, and also suppose  $\lambda_C$  is an eigen value of matrix C that is assumed diagonalized to  $\Lambda_C$  by orthogonal transform Q as  $C = Q \Lambda_C Q^T$ .

When a matrix  $(A+C)$  has an eigen value  $\lambda$  as  $(A+C)x = \lambda x$ , since  $(Q^T A Q)x = (\lambda - \lambda_c)x$ ,  $A(Qx) = (\lambda - \lambda_c)(Qx)$  results. And this implies  $\lambda = \lambda_A + \lambda_c$ .

It should be noted that in the system  $\dot{\hat{x}} = \{\Theta A \Theta^T - [\omega]\} \hat{x} + \Theta B u = \hat{A}(t)\hat{x} + \hat{B}(t)u$ ,  $[\omega]$  has the eigen values of pure imaginary and is diagonalized by orthogonal transformation. Thus the transfer function  $G(s) = (sI - A)^{-1} B$  shifts its poles of the transfer function  $\hat{G}(s) = (sI - \hat{A})^{-1} B$  in C-W coordinate to higher frequency direction. This causes the performance index distinction between C-W and Inertial coordinates.

### Case-2 : Performance Index Evaluation

Here is evaluated the performance under the following index, for the controller designed in autonomous (C-W) coordinate.

$$\hat{J} = \int_0^\infty \left( \frac{1}{2} x^T Q(t)x + \frac{1}{2} u^T R u \right) = \frac{1}{2} x(t_0)^T S(t_0)x(t_0), \quad Q(t) = \Theta(t)^T \hat{Q} \Theta(t) \quad (21)$$

The performance index is obtained by solving the following equation with a pre-determined gain  $K(t)$ :

$$-\dot{S} = (A - BK(t))^T S + S(A - BK(t)) + K(t)^T R K(t) + Q(t), \quad S(\infty) = 0 \quad (22)$$

While the gain  $K_0$  is designed in C-W coordinate based on

$$-\dot{S}_0 = 0 = (A - BK_0)^T S_0 + S_0(A - BK_0) + K_0^T R K_0 + Q_0 \quad K_0 = R^{-1} B^T S_0 \quad (23)$$

the evaluation results in solving

$$-\dot{S} = (A - BK_0)^T S + S(A - BK_0) + K_0^T R K_0 + Q(t), \quad S(\infty) = 0 \quad (24)$$

And the performance difference is obtained by

$$-(\dot{S} - \dot{S}_0) = (A - BK_0)^T (S - S_0) + (S - S_0)(A - BK_0) + (Q(t) - Q_0) \quad (25)$$

In case the last term in the equation above is positive definite, the performance difference is positive and this means the performance is degrade. The astronomy pointing performance is defined in Inertial Coordinate, and it is obviously directional, and is not described as a constant weighting in C-W coordinate. Thus designing in Inertial Coordinate must be better for the astronomy purpose.

Note, in case a Time-Varying weighting is introduced in C-W coordinate, the design results in the same performance and the same gain. But such design process is identical to design in Inertial Coordinate.

### Formation maintenance property

Fig. 3 shows a schematic drawing of three coordinates to be discussed. The control schemes for the formation maintenance rely on the observation measurements with the other spacecraft among the formation. Sometimes, Hill's equations are utilized to describe the relative motion. But it is not directly related to the formation geometry. In most cases, the spacecraft attitude regardless of whether it is a chaser or evader, what is readily available does not appear intimately as long as C-W description is used. The relative motion seen in the inertial coordinate is not simple but complicated as in the figure. On the Hill's coordinate, such closed loci relative motions are along virtual ellipses, and the motion is simple enough. However, what is readily available aboard the spacecraft shows almost frozen geometry, while the motion description needs expressed in a not-straightforward manner as on the Hill's coordinate. While the formation is completely frozen, the Hill's state vectors are not frozen. As this implies, the use of inertial coordinate has some practical advantage. On the p-coordinate introduced here, the measurements are nearly the direct observation information obtained on the spacecraft to the adjacent spacecraft. On a complete frozen formation, the p-coordinate presents a frozen constant vector. And it apparently looks similar to the relative motion in the inertial motion.

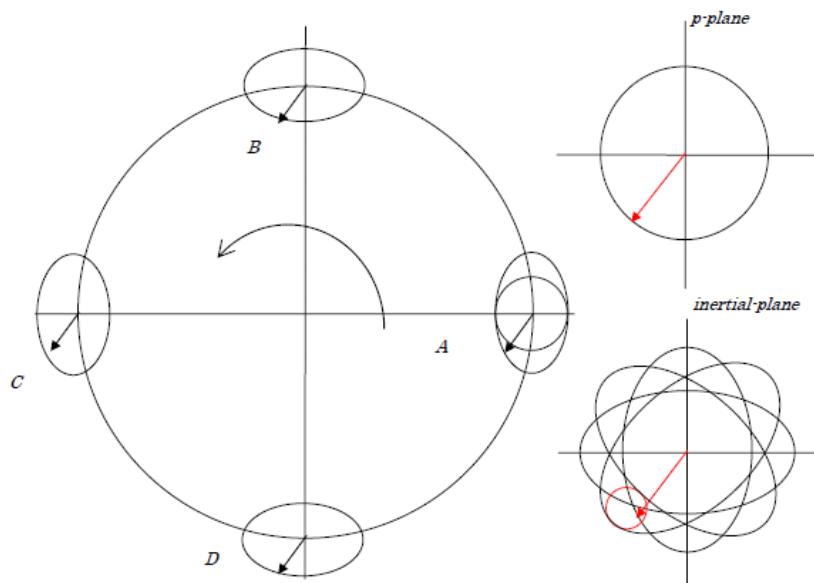


Fig. 3: Measurements Properties and  $p$ -Coordinate and Inertial Coordinate

### 3.3 Comparison of Hill's (C-W), Inertial and $p$ -coordinates

So far, the paper has discussed about how non-autonomous systems work and what kind of distinction appears. What follows summarizes the characteristics of it.

- Formation measurement does not relate to the Hill's coordinate, since in most cases the spacecraft is stabilized in three-axis manner.



- Inertial frame is useful as for astronomy missions in this regard. But the relative motion is always varying even though the formation gets settled to natural trajectories.
- $p$ -coordinate retains measurement characteristics and shows the frozen property for settled formation.

**Table 1 Summary of Comparison among C-W, Inertial and  $p$ -Coordinates**

	C-W (Hill's)	Inertial	$p$ -coordinate
Eq. of Motion	Available	Available	Available
Time-Invariance	Invariant	Variant	Variant
Analytic solutions	Available	Available	Available
Observability*	Not Appropriate	Appropriate	Suitable
Formation Target	Time-Varying	Time-Varying	Frozen
Steady State Control Input	Persistently Varying	Persistently Varying	Zero
Appropriate for	NADIA Tracking	Astronomy	Formation Maintenance
Advantage	Comprehensive Stability Augmentation	Minimizes suitable Performance Index	Defines a specific bin/slot easily that each s/c to be controlled

#### 4. Formation design around elliptical orbit using the levi-civita coordinate transformation

##### 4.1 Levi-Civita Coordinate Transformation

What this paper aims at is eliminating the restoring terms from the equations of motion, so that the resulted equation automatically can include the steady state target vector in it. The generalized Hill's equation which is applicable to circular and elliptical orbits is written as follows:

$$\begin{aligned}
 \ddot{\hat{x}} - 2\omega\dot{\hat{y}} - \left(1 + \frac{2r}{p}\right)\omega^2\hat{x} - \dot{\omega}\hat{y} &= u_x \\
 \ddot{\hat{y}} + 2\omega\dot{\hat{x}} - \left(1 - \frac{r}{p}\right)\omega^2\hat{y} + \dot{\omega}\hat{x} &= u_y \\
 \ddot{\hat{z}} + \frac{r}{p}\omega^2\hat{z} &= u_z
 \end{aligned} \tag{26}$$

The paper has indicated the possible coordinate transformation by which the restoring terms can vanish. However, specific manipulation is not rewarded enough. When we look at the original two bodies motion generally, which is applicable widely for ellipses, it is written as:

$$\ddot{\mathbf{r}} + \frac{\mu}{r^3}\mathbf{r} = \mathbf{0} \tag{27}$$

And here is introduced the coordinate transformation of  $\frac{ds}{dt} = \frac{1}{r}$ . It is the Levi-Civita transformation. When we now confine our discussion to the planar motion, the introduction of

$$\begin{pmatrix} x_1 \\ x_2 \end{pmatrix} = \begin{pmatrix} u_1^2 - u_2^2 \\ 2u_1u_2 \end{pmatrix} = \begin{pmatrix} u_1 & -u_2 \\ u_2 & u_1 \end{pmatrix} \begin{pmatrix} u_1 \\ u_2 \end{pmatrix} \equiv L(u)u \quad (28)$$

$$L(u) = \begin{pmatrix} u_1 & -u_2 \\ u_2 & u_1 \end{pmatrix} \quad (29)$$

makes the equations of motion to

$$u'' + \left(-\frac{h}{2}\right)u = u'' + \Omega^2 u = 0 \quad (30)$$

Here  $h = \frac{1}{2} \frac{|r'|^2}{r^2} - \frac{\mu}{r}$  and the operator of  $(\square)' \equiv \frac{d}{ds}(\square)$  is introduced. The use of this Levi-Civita transformation converts the equations of motion into linear ordinary equations of motion as above. The fictitious independent variable  $s$  relates to the eccentric anomaly  $E$  as  $\Omega s = \frac{E}{2}$  and the solution is expressed as:

$$u = \begin{pmatrix} \alpha \cos \frac{E}{2} \\ \beta \sin \frac{E}{2} \end{pmatrix} \quad (31)$$

The independent variable is replaced hereafter as  $E$  and  $\dot{E} = \frac{an}{r}$  holds.

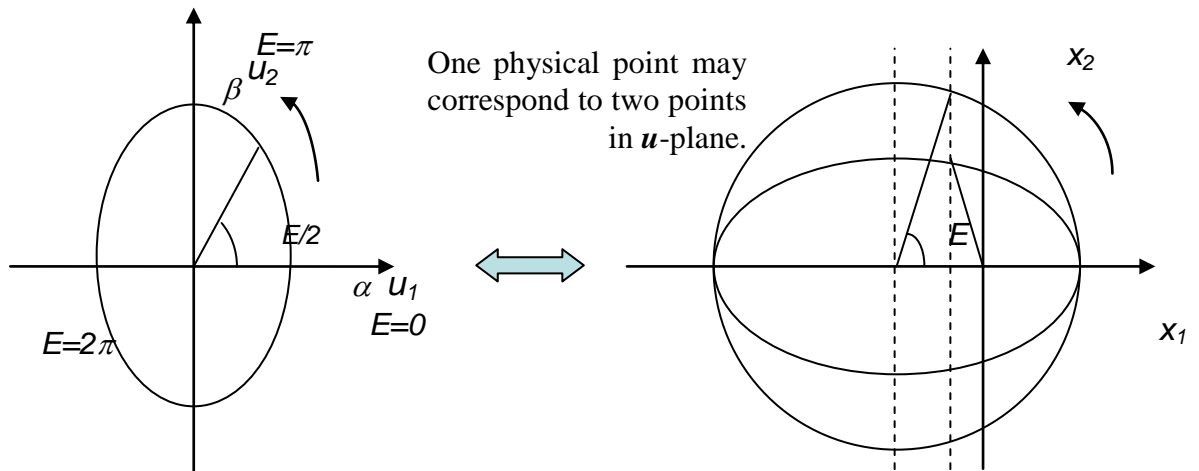


Fig. 4: The Levi-Civita Coordinate Transformation and Linearization

Note the variation  $\delta u$  does not satisfy the same equations since the new independent variable  $s$

does not grow up in the same rate between multiple separated satellites. Though the motion can be described very simple in the u-plane, some measures should be taken to compensate for the deviation of the independent variables between multiple satellites.

#### 4.2 Derivation of Basic Equations for the Formation Design

Here the situation where a mother satellite (“satellite 1”) is flying in an elliptical orbit and a daughter satellite (“satellite 2”) is flying near the mother. The mother crosses its perigee at time  $t = 0$  or  $s_1 = 0$ . The trajectory of the mother  $u_1$  is expressed as:

$$u_1 = \begin{pmatrix} \alpha \cos \frac{E_1}{2} \\ \beta \sin \frac{E_1}{2} \end{pmatrix} \quad (32)$$

Here,  $\alpha < \beta$  in order that  $E_1=0$  corresponds to the perigee.

The deviation of the daughter relative to the mother can be expressed using the following three parameters (Fig. 5).

1. Deviation of eccentric anomaly  $\Delta E$  of the daughter relative to the mother at time  $t = 0$ . It is assumed that the daughter crosses its perigee at  $s_2 = 0$  or  $E_2=0$  ( $t$  is not zero).
2. The difference of the eccentricity  $\Delta e$  between the daughter’s orbit and the mother’s.
3. The angular difference of the direction of perigee  $\theta$

It is assumed that the semi-major axis  $a$  of the daughter is the same as that of the mother. This implies that the period of the orbit is the same. Otherwise, the daughter will drift from the mother as time passes and the formation will collapse.

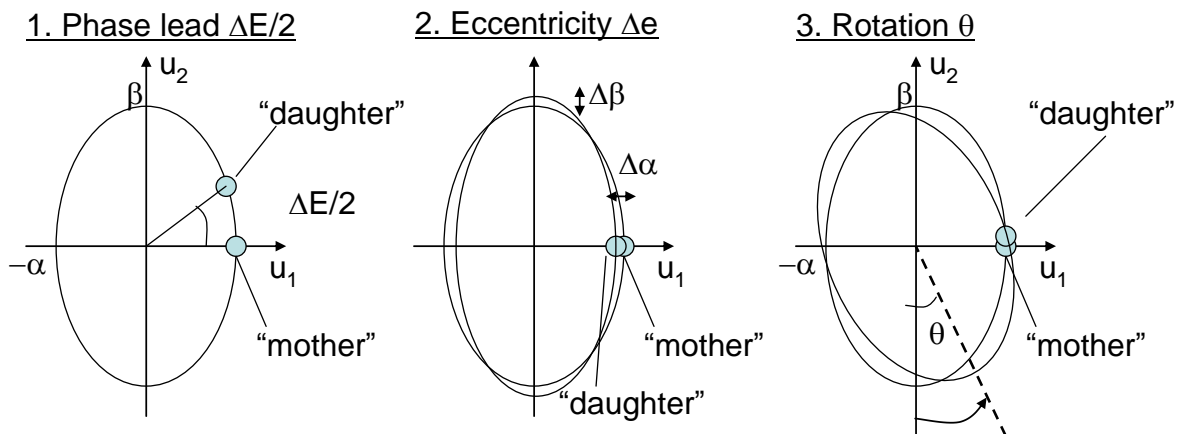


Fig. 5: Three types of orbital deviation

The effect of these three parameters on the motion of the daughter can be expressed by the

difference of eccentric anomaly  $E$  and geometrical parameter ( $\alpha$  and  $\beta$ ) of the daughter from the mother. The relation is derived in the following section. It is also assumed that  $\Delta E, \Delta e, \theta \ll 1$ .

#### Effect of $\Delta E$

When initial displacement of eccentric anomaly  $\Delta E$  is applied to the daughter at time  $t = 0$ ,  $\Delta E_1 \ll E_2 - E_1$  does not keep constant for  $t$  or  $E_1$ . Considering the Kepler equation  $E - e \sin(E) = n^* t$ , the difference of the eccentric anomaly  $\Delta E_1$  between the daughter and the mother varies and is approximately expressed using  $E_1$  and the initial displacement  $\Delta E$ :

$$\Delta E_1 = \frac{1-e}{1-e \cos E_1} \Delta E \quad (33)$$

#### Effect of $\Delta e$

When the eccentricity of the daughter's orbit is deviated,  $\alpha$  and  $\beta$  as well as  $E_2$  is affected. The deviation of these parameters is calculated using geometrical relation between  $\alpha$ ,  $\beta$  and  $e$  and also the Kepler equation:

$$\Delta \alpha = -\frac{(\alpha^2 + \beta^2)}{4\alpha} \Delta e \quad (34)$$

$$\Delta \beta = \frac{(\alpha^2 + \beta^2)}{4\beta} \Delta e \quad (35)$$

$$\Delta E_2 = \frac{\sin E_1}{1-e \cos E_1} \Delta e \quad (36)$$

When the above two parameters are applied, the motion of the daughter is expressed as follows:

$$\mathbf{u}_2 = \begin{pmatrix} (\alpha + \Delta \alpha) \cos \frac{1}{2}(E_1 + \Delta E_1 + \Delta E_2) \\ (\beta + \Delta \beta) \sin \frac{1}{2}(E_1 + \Delta E_1 + \Delta E_2) \end{pmatrix} \quad (37)$$

#### Effect of $\theta$

Finally, the rotation of the direction of the perigee  $\theta$  is applied,

$$\begin{aligned} \mathbf{u}_2 &\leftarrow \begin{pmatrix} \cos \theta & -\sin \theta \\ \sin \theta & \cos \theta \end{pmatrix} \mathbf{u}_2 \approx \begin{pmatrix} 1 & -\theta \\ \theta & 1 \end{pmatrix} \mathbf{u}_2 \\ &= \begin{pmatrix} (\alpha + \Delta \alpha) \cos \frac{E_1}{2} - \frac{\alpha}{2} (\Delta E_1 + \Delta E_2) \sin \frac{E_1}{2} - \beta \theta \sin \frac{E_1}{2} \\ \alpha \theta \cos \frac{E_1}{2} + (\beta + \Delta \beta) \sin \frac{E_1}{2} + \frac{\beta}{2} (\Delta E_1 + \Delta E_2) \cos \frac{E_1}{2} \end{pmatrix} \end{aligned} \quad (38)$$

And the relative position of the daughter in the  $u$ -plane is expressed as:

$$\delta \mathbf{u} = \begin{pmatrix} \Delta \alpha \cos \frac{E_1}{2} - \frac{\alpha}{2} (\Delta E_1 + \Delta E_2) \sin \frac{E_1}{2} - \beta \theta \sin \frac{E_1}{2} \\ \alpha \theta \cos \frac{E_1}{2} + \Delta \beta \sin \frac{E_1}{2} + \frac{\beta}{2} (\Delta E_1 + \Delta E_2) \cos \frac{E_1}{2} \end{pmatrix} \quad (39)$$

When eqs. (34) – (36) are substituted, the relative motion of the daughter in the u-plane is obtained as a function of the three parameters  $\Delta E, \Delta e, \theta$ :

$$\delta \mathbf{u} = \begin{pmatrix} - \left( \frac{(\alpha^2 + \beta^2)}{4\alpha} \cos \frac{E_1}{2} + \frac{\alpha \sin E_1 \sin \frac{E_1}{2}}{2(1 - e \cos E_1)} \right) \Delta e - \beta \sin \frac{E_1}{2} \theta - \frac{\alpha(1 - e) \sin \frac{E_1}{2}}{2(1 - e \cos E_1)} \Delta E \\ \alpha \cos \frac{E_1}{2} \theta + \left( \frac{(\alpha^2 + \beta^2)}{4\beta} \sin \frac{E_1}{2} + \frac{\beta \sin E_1 \cos \frac{E_1}{2}}{2(1 - e \cos E_1)} \right) \Delta e + \frac{\beta(1 - e) \cos \frac{E_1}{2}}{2(1 - e \cos E_1)} \Delta E \end{pmatrix} \quad (40)$$

This equation is the basis for the formation design.

### 4.3 Design of Pseudo-Constant Distant Formation for Elliptical Orbit

In this section, pseudo-constant distant formation for elliptical orbit is designed using the basic equations derived above.

By differentiating the eq.(28), relative position in the physical plane  $\delta \mathbf{r} = \mathbf{r}_2 - \mathbf{r}_1$  can be expressed by the relative position in the u-plane  $\delta \mathbf{u} = \mathbf{u}_2 - \mathbf{u}_1$  and  $\mathbf{u}_1$  :

$$\delta \mathbf{r} \approx 2\mathbf{L}(\mathbf{u}_1)\delta \mathbf{u} \quad (41)$$

so that the relative distance between the daughter and the mother is

$$|\delta \mathbf{r}|^2 = \delta \mathbf{r}^T \delta \mathbf{r} \approx 4\delta \mathbf{u}^T \mathbf{L}(\mathbf{u}_1)^T \mathbf{L}(\mathbf{u}_1)\delta \mathbf{u} = 4|\mathbf{u}_1|^2 |\delta \mathbf{u}|^2 \quad (42)$$

where  $\mathbf{L}(\mathbf{u}_1)^T \mathbf{L}(\mathbf{u}_1) = |\mathbf{u}_1|^2 \mathbf{I}$ . For the relative distance to be constant, the following relation should hold:

$$|\delta \mathbf{r}|^2 = const \Leftrightarrow |\mathbf{u}_1|^2 |\delta \mathbf{u}|^2 = const \Leftrightarrow |\mathbf{r}_1| |\delta \mathbf{u}|^2 = const \Leftrightarrow \frac{|\delta \mathbf{u}|^2}{1 + e \cos E_1} = const \quad (43)$$

Note that the formation  $|\delta \mathbf{u}| = const$  achieves constant distance  $\delta \mathbf{r}$  in case the reference orbit is circular ( $e = 0$ ).

When we now confine the discussion to the case  $\Delta e = 0$ , relative motion of the daughter in the u-plane becomes:

$$\delta u(1) = \begin{pmatrix} -\beta \sin \frac{E_1}{2} \theta - \frac{\alpha(1-e) \sin \frac{E_1}{2}}{2(1-e \cos E_1)} \Delta E \\ \alpha \cos \frac{E_1}{2} \theta + \frac{\beta(1-e) \cos \frac{E_1}{2}}{2(1-e \cos E_1)} \Delta E \end{pmatrix} \quad (44)$$

And when the approximation  $\frac{1}{1-e \cos E_1} \approx \frac{1+e \cos E_1}{1-e^2}$  is applied,

$$\delta u(1) = \begin{pmatrix} -\sin \frac{E_1}{2} \left( \beta \theta + \frac{\alpha \Delta E (1+e \cos E_1)}{2(1+e)} \right) \\ \cos \frac{E_1}{2} \left( \alpha \theta + \frac{\beta \Delta E (1+e \cos E_1)}{2(1+e)} \right) \end{pmatrix} \quad (45)$$

Taking into consideration that  $\delta u$  is the linear sum of  $\Delta E, \theta$ , we can redefine  $\Delta E$  as  $\Delta E \square \Delta E / \theta$ .

Note that  $\Delta E \square 1$  does not hold for the new  $\Delta E$ . Using this new definition  $\Delta E$ ,

$$\delta u(1) / \theta = \begin{pmatrix} -\sin \frac{E_1}{2} \left( \beta + \frac{\alpha \Delta E (1+e \cos E_1)}{2(1+e)} \right) \\ \cos \frac{E_1}{2} \left( \alpha + \frac{\beta \Delta E (1+e \cos E_1)}{2(1+e)} \right) \end{pmatrix} \quad (46)$$

so that

$$\begin{aligned} \frac{\delta u(1)^2 + \delta u(2)^2}{\theta^2} &= \sin^2 \frac{E_1}{2} \left( \beta + \frac{\alpha \Delta E (1+e \cos E_1)}{2(1+e)} \right)^2 + \cos^2 \frac{E_1}{2} \left( \alpha + \frac{\beta \Delta E (1+e \cos E_1)}{2(1+e)} \right)^2 \\ &= \alpha^2 \cos^2 \frac{E_1}{2} + \beta^2 \sin^2 \frac{E_1}{2} + \alpha \beta \Delta E \frac{1+e \cos E_1}{1+e} + \frac{(1+e \cos E_1)^2}{4(1+e)^2} \Delta E^2 (\beta^2 \cos^2 \frac{E_1}{2} + \alpha^2 \sin^2 \frac{E_1}{2}) \\ &= a(1-e \cos E_1) + a \sqrt{1-e^2} \Delta E \frac{1+e \cos E_1}{1+e} + a(1+e \cos E_1)^3 \frac{\Delta E^2}{4(1+e)^2} \end{aligned} \quad (47)$$

Here, we define  $x \square e \cos E_1$  ( $-e < x < e$ ),

$$\frac{\delta u(1)^2 + \delta u(2)^2}{a \theta^2} = (1-x) + \sqrt{1-e^2} \Delta E \frac{1+x}{1+e} + (1+x)^3 \frac{\Delta E^2}{4(1+e)^2} \quad (48)$$

For the relative distance to be (pseudo-) constant, the following function  $f(x)$  should be (pseudo-) constant for all  $x$  ( $-e < x < e$ ):

$$f(x) \square \frac{\delta u(1)^2 + \delta u(2)^2}{a \theta^2} / (1+x) = \frac{1-x}{1+x} + \frac{\sqrt{1-e^2}}{1+e} \Delta E + (1+x)^2 \frac{\Delta E^2}{4(1+e)^2} \quad (49)$$

It can be derived that the variation of  $f(x)$  is minimum if  $f(x)$  takes its local minimum at  $x = 0$ , or  $f'(0) = 0$ . This leads to  $\Delta E^2 = 4(1+e)^2$  and remembering the definition of the new  $\Delta E$ , the pseudo-constant distance formation can be achieved when:

$$\Delta E = 2(1+e) \quad (50)$$

#### 4.4 Numerical Verification of the Formation Design

Here, the above formation design is verified by numerical simulations. The orbit of the mother is set so that the apogee altitude is 8000[km] and the perigee altitude 600[km]. The eccentricity  $e$  is 0.3465. Numerical simulations are done in such a way that the motion of the mother and the daughter is propagated using eq.(27), and the ratio of minimum distance to maximum distance is evaluated which we call “constant distance ratio”. The initial condition for the daughter  $r_2, \dot{r}_2, u_2, u_2'$  is generated through  $\Delta E, \theta$ .

Fig. 6 shows the constant distance ratio for  $\Delta E, \theta$ . The horizontal axis is  $\theta$ , the vertical axis  $\Delta E$ , and the color corresponds to the constant distant ratio. The value of  $\Delta E, \theta$  is selected in the range  $0 < \Delta E < 0.1$  [rad] and  $|\theta| < 0.05$  [rad]. The figure indicates that the constant distance ratio is maximum along a line  $\Delta E/\theta = const$  and the gradient well corresponds to eq.(50), and 95% of constant distance ratio was achieved, which is also shown in the time history of relative distance (Fig. 7).

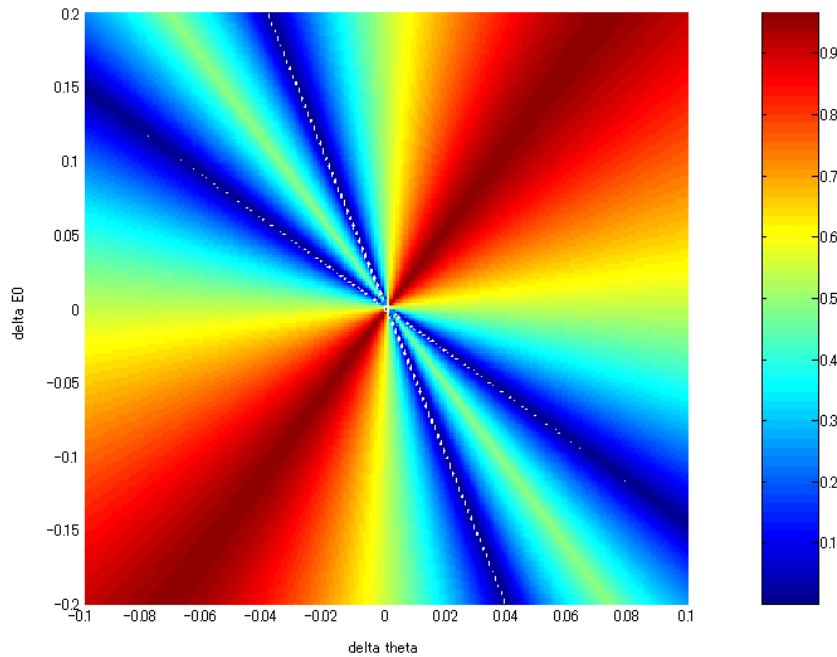


Fig. 6: Constant distant ratio for  $e=0.3$

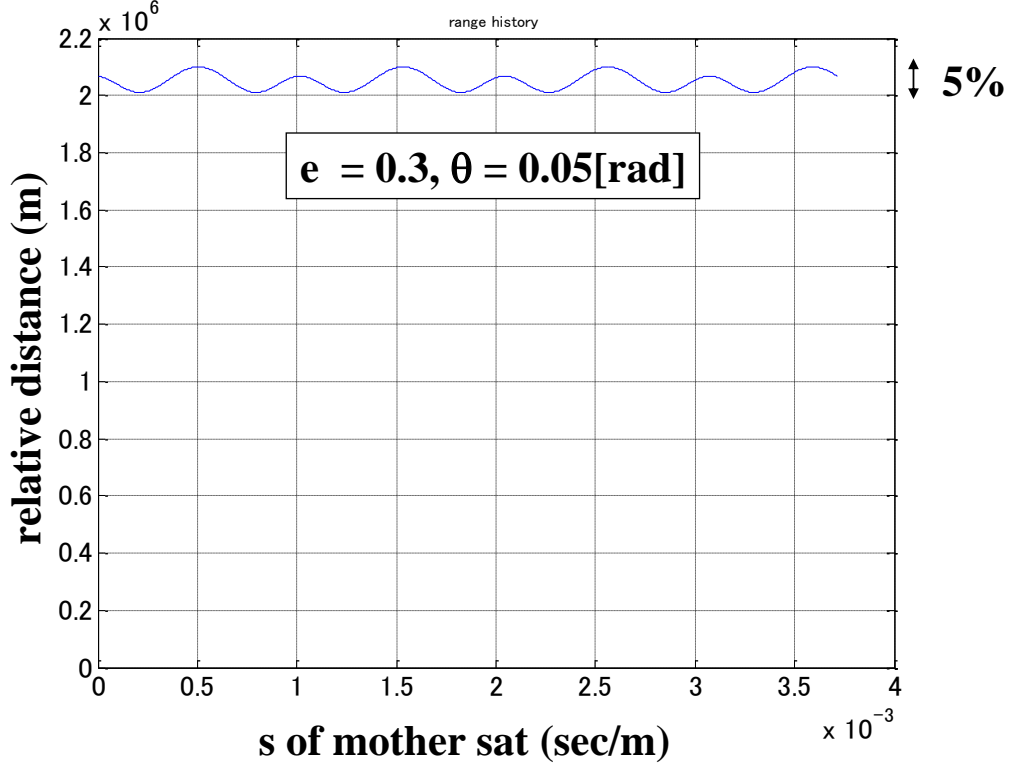


Fig. 7: Relative distance history for  $e=0.3$

#### 4.5 Design of Constant Angular Separation Formation for Elliptical Orbit

Here, we consider another daughter satellite (“satellite 3”) for the design of “constant angular separation” formation. The angular separation is defined as the angular difference between the direction from satellite 1 to satellite 2 and that from satellite 1 to satellite 3, or the angle of satellite 3 – satellite 1 – satellite 2. Relative position vector of satellite 2 and 1  $\delta \mathbf{r}_2 = \mathbf{r}_2 - \mathbf{r}_1$  and that of satellite 3 and 1  $\delta \mathbf{r}_3 = \mathbf{r}_3 - \mathbf{r}_1$  is expressed as:

$$\begin{aligned}\delta \mathbf{r}_2 &= 2\mathbf{L}(\mathbf{u}_1)\delta \mathbf{u}_2 \\ \delta \mathbf{r}_3 &= 2\mathbf{L}(\mathbf{u}_1)\delta \mathbf{u}_3\end{aligned}\quad (51)$$

So, the angular separation  $\phi$  is calculated as:

$$\cos \phi = \frac{\delta \mathbf{r}_2^T \delta \mathbf{r}_3}{|\delta \mathbf{r}_2| |\delta \mathbf{r}_3|} = \frac{4\delta \mathbf{u}_2^T \mathbf{L}(\mathbf{u}_1)^T \mathbf{L}(\mathbf{u}_1) \delta \mathbf{u}_3}{4|\delta \mathbf{u}_2| |\mathbf{u}_1| |\delta \mathbf{u}_3| |\mathbf{u}_1|} = \frac{\delta \mathbf{u}_2^T \delta \mathbf{u}_3}{|\delta \mathbf{u}_2| |\delta \mathbf{u}_3|} = \cos \phi_u \quad (52)$$

where  $\phi_u$  denotes the angular separation in the  $u$ -plane. This indicates that the “constant angular separation” formation can be designed so that the angular separation in the  $u$ -plane is kept constant.



## 5. Conclusion

This paper first discussed the appropriate coordinate expression for different kind of formation flying missions, where a formation around circular orbit is assumed and three different coordinates are presented; 1) C-W coordinate, 2) Inertial coordinate and 3) p-coordinate. Although the three coordinates are similar in terms of controller stability, the p-coordinate is shown effective for a formation maintenance control where each spacecraft is moving on a locus in the C-W coordinate, in terms of control performance index and formation maintenance property.

Then, the discussion is extended to the formation around general elliptic orbit. The design of formation is not so simple as for the case of circular trajectory. In this paper, formation design strategy around elliptical orbit was derived through the regularization technique and Levi-Civita coordinate transformation. As an example, constant distant formation around elliptical orbit was derived analytically and the strategy was also verified through numerical simulations. The results can lead to the derivation of another generalized p-coordinate for the case of elliptic reference orbit.

This paper encourages engineers to visit non-autonomous coordinates in some practical applications rather than resorting to the C-W coordinates.

## References

1. Kawaguchi, J. and Mizuta H., A Relayed Formation Flying Control with Analogy Discussion to Traffic System, IAC-06- C1.8.2, Valencia, Oct. 2-6, 2007.
2. Kawaguchi, J. Modified Equations of Motion around Circular Trajectory and its Application to Formation Flying Control, AAS 07-110, AAS Flight Mechanics Conference, Sedona, AZ, Jan 30-Feb. 1, 2007
3. Roberts, J., <https://aerade.cranfield.ac.uk/bitstream/1826/1114/1/J+Roberts+PhD.pdf>
4. Schweighart, S.A. and Sedwick, R.J. (2001a), 'Development and Analysis of a High Fidelity Linearized J2 Model for Satellite Formation Flying', AIAA Space 2001: Conference and Exposition, Albuquerque, New Mexico, AIAA 2001-4744.
5. Schweighart, S.A. and Sedwick, R.J. (2002), 'High-Fidelity Linearized J2 Model for Satellite Formation Flight', Journal of Guidance, Control and Dynamics, Vol. 25, No. 6, pp. 1073-1080.

## **Authors**

R. Funase, Institute of Space and Astronautical Science (ISAS), Japan Aerospace Exploration Agency (JAXA), Japan, Tokyo Denki University, Japan

Contacts: 3-1-1 Yoshinodai, Sagamihara 229-8510, Japan, [funase@isas.jaxa.jp](mailto:funase@isas.jaxa.jp)

J. Kawaguchi, Institute of Space and Astronautical Science (ISAS), Japan Aerospace Exploration Agency (JAXA), Japan, Tokyo Denki University, Japan

Contacts: 3-1-1 Yoshinodai, Sagamihara 229-8510, Japan